Available online at www.sciencedirect.com
SCIENCE DIRECT®
ELSEVIER
Journal of Magnetism and Magnetic Materials 293 (2005) 320–327
Journal of magnetism and magnetic materials
www.elsevier.com/locate/jmmm

Temperature change of various ferrite particles with alternating magnetic field for hyperthermic application

Dong-Hyun Kim[a,b], Se-Ho Lee[a,b], Kyoung-Nam Kim[a,b], Kwang-Mahn Kim[a,b], In-Bo Shim[c], Yong-Keun Lee[a,b,*]

[a]*Brain Korea 21 Project for Medical Science, Yonsei University College of Dentistry, Seoul 120-752, Republic of Korea*
[b]*Department and Research Institute of Dental Biomaterials and Bioengineering, Yonsei University College of Dentistry, Seoul 120-752, Republic of Korea*
[c]*Department of Electronic Physics, Kookmin University, Seoul 136-702, Republic of Korea*

Available online 29 March 2005

Abstract

Various ferrites (Fe-, Li-, Ni/Zn/Cu-, Co-, Co/Ni, Ba- and Sr-ferrites) were investigated with respect to their application for hyperthermia. Temperature changes under an alternating magnetic field were observed. The area of hysteresis loop was much larger in the Ba- and Sr-ferrites than for that of the Fe-, Ni/Zn/Cu-, Li-, Co- and Co/Ni-ferrites. Co-ferrite exhibited the most applicable temperature change $\Delta T = 19.25\,\mathrm{K}$ ($29.62\,\mathrm{W/g\,s}$), in distilled water when the field was 110 A/m.

PACS: 75.50.G; 87.54.B; 76.60.E

Keywords: Ferrite; Hyperthermia; Hysteresis loss; AC magnetic field; CoNi ferrite; Co ferrite; NiZnCu ferrite; Ba ferrite; Sr ferrite

1. Introduction

Thermal energy from a hysteresis loss of ferrites depends on the type of the remagnetization process. Over certain portions the magnetization curve (B versus H, where B is the magnetic induction through the material and H is the applied external field) is irreversible and energy is dissipated into the medium with each flux-reversal cycle in the form of heat. For the reversible processes, energy is stored in the lattice just as potential energy is stored in a spring that is compressed by an external force. For the irreversible processes, energy is dissipated as heat with the additional degrees of freedom that are excited in the lattice [1]. The actual physical processes by which energy is dissipated in the course of a quasistatic traversal of the hysteresis loop are

*Corresponding author. Tel.: +82 2 361 8063; fax: +82 2 364 9961.
E-mail address: leeyk@yumc.yonsei.ac.kr (Y.-K. Lee).

0304-8853/$ - see front matter © 2005 Published by Elsevier B.V.
doi:10.1016/j.jmmm.2005.02.077

identical with those responsible for the dynamic losses. The energy per unit volume of a magnetic material of magnetization M in an external field H is given by $-HM$. Therefore, the sum of the energy stored and the heat dissipated in a magnetic material whose magnetization changes from $M1$ to $M2$ when placed in a magnetic field H is [2]

$$W = \int_{M1}^{M2} H \, \mathrm{d}M.$$

Hyperthermia is a cancer treatment modality that destroys tumors by elevating the temperature of the cancerous tissue to approximately 43 °C for 20–60 min [3]. The temperature in tumor tissues rises much easier than in normal tissues because the tumor tissues have a higher heat sensitivity and a smaller cooling effect due to their blood flow. Hyperthermia is a therapeutic technique that is used against tumors for a small percentage of patients in the conjunction with other techniques such as surgical operation, chemotherapy and radiotherapy. However, the hyperthermia is expected in the future to be one of the most important treatments for many kinds of cancer.

Considering the method of heating, hyperthermia can be divided into three broad categories: whole body hyperthermia, regional hyperthermia and local hyperthermia. In the first two methods, a rising temperature is induced over a general volume containing the tumor. In local hyperthermia a focused heating is performed. The latter mentioned method is often preferred, since the capability of heating only the desired volume (tumor) without affecting the surrounding tissue is more ideal [4]. One of the most promising methods of localized hyperthermia is locating exothermic ferrite particles at the tumor site and then radiating this volume with AC magnetic fields. The cornerstone for the broad and reliable clinical use of hyperthermia in cancer treatment is a heat delivery technique that must provide a controlled, local thermal effect within the whole mass of the cancerous tissue while leaving normal tissues unaffected. Moreover, the technique as well must deliver the heat systemically to a tumor deep within the body. To meet these requirements, several ferrite particles have been proposed as medical tools to produce hyperthermia of tumors [5]. Therefore, knowing the heating characteristics of various particles will enhance cancer treatment planning and the experimental verification of the different ferrite particles. For use as a hyperthermic thermoseed, the specific loss power (SLP) in alternating magnetic field, as the main parameter characterizing the ferrite particle, has to be investigated thoroughly [6]. In this study, various ferrite particles with different magnetic properties were prepared with the sol–gel method and their heating properties were measured by a heating system using an alternating magnetic field generator and amplifier.

The purpose of this study was to assess the applicability of ferrite particles for their hysteresis loss in heating hyperthermia at various frequencies.

2. Experimental

We synthesized the ferrite particles by sol–gel ($Ni_{0.65}Zn_{0.35}Cu_{0.1}Fe_{1.9}O_4$, $Li_{0.5}Fe_{2.5}O_4$, $Co_{1-x}Ni_xFe_2O_4$, $Ba_{1-x}Sr_xFe_{12}O_{19}$) and coprecipitation ($Fe_3O_4$). First, an aqueous suspension of $Fe(OH)_2$ was prepared by adjusting the pH of a $FeCl_2$ aqueous solution to 7.8 and then H_2O_2 was added to promote the oxidation to Fe_3O_4. We also synthesized $Li_{0.5}Fe_{2.5}O_4$, $Ni_{0.65}Zn_{0.35}Cu_{0.1}Fe_{1.9}O_4$ particles by the same sol–gel route. Weighed amounts of $Ni(CH_3CO_2)_2 \cdot 4H_2O$ (Sigma, USA), $Zn(NO_3)_2 \cdot 6H_2O$ (Sigma, USA), $Cu(CH_3CO_2)_2 \cdot 4H_2O$ (Sigma, USA), $Fe(NO_3)_3 \cdot 9H_2O$ (Sigma, USA), $Li(C_2H_3O_2) \cdot 2H_2O$ (Sigma, USA) were first dissolved in 2-methoxyethanol, diethanolamine and water for 30 min by the use of an ultrasonic cleaner. The solution was refluxed at 70 °C for 12 h to allow the gel formation, and then it was dried at 100 °C in a dry oven for 24 h and next fired at 800 °C for 6 h in air. $Co(CH_3CO_2)_2 \cdot 4H_2O$, $Ni(CH_3CO_2)_2 \cdot 4H_2O$, and $Fe(NO_3)_3 \cdot 9H_2O$ were selected as precursors of $Co_{1-x}Ni_xFe_2O_4$ ferrite. They were dissolved in acetic acid, methanol and DI water and stirred for 1 h. This solution was refluxed at room temperature for 24 h to allow gel formation, dried at 100 °C for 24 h and then fired at 800 °C for 6 h in air. Besides, $Ba(NO_3)_2$, $Sr(CH_3CO_2)_2$, and

$Fe(NO_3)_3 \cdot 9H_2O$ were used to synthesize $Ba_{1-x}Sr_xFe_{12}O_{19}$ ferrite. They were dissolved in ethylene glycol, methyl alcohol and DI water, refluxed at 80 °C for 12 h and then fired at 1000 °C for 6 h in air. The crystalline phases of ferrite sample were identified from an X-ray diffractometer (XRD; D/MAX Rint 2000, Rigaku, Japan) using CuKα radiation. A vibrating sample magnetometer (VSM; 7300 Lakeshore, USA) was used to measure the saturation magnetization as well as the coercive force. The size of ferrite particles was determined using scanning electron microscope (SEM; S2700, Hitachi, Japan) observation.

The heating system consists of four main subsystems; a variable frequency and amplitude sine wave function generator (15 MHz/20 Vp-p, G5100, USA), a power amplifier (DC 10 MHz/142 Vp-p, HAS4101, USA), an induction coil (length: 30 m, turns: 43, diameter: 172 mm, height: 320 mm) and an oscilloscope (Goldstar, Korea), temperature controller (1.4−1000 K, Lake shore, USA) (Fig. 1).

The coil consisted of loops of copper pipe and the copper pipe was cooled by water to keep its temperature constant. The temperature of the water was monitored using a thermocouple, and this was followed by placing the prepared ferrite particles into a PCR micro tube filled with 0.2 ml of DI water (the particles were completely immersed) and the samples were subjected to various frequencies and voltages of an alternating magnetic field. The near-adiabatic chamber consisted of densely packed Styrofoam walls and bottom. The thermocouple was positioned in the DI water and the center of coil was without contact to the ferrite particles. An alternating magnetic field was applied to the samples using this coil, and the magnetic field was applied for a given amount of time and then turned off.

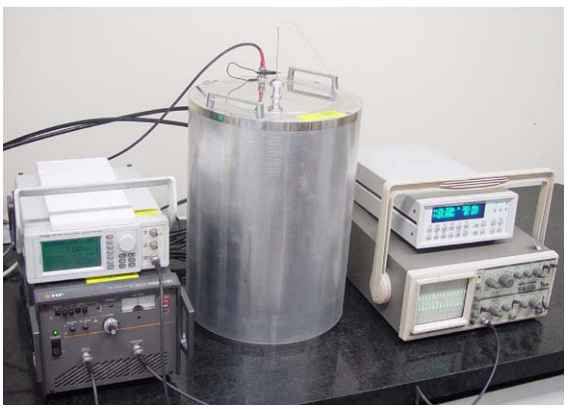

Fig. 1. Photograph of our alternating magnetic field apparatus.

Using a bandwidth function generator system, the temperature changes under an alternating magnetic field of various frequencies were observed. The SLP of the ferrite particles in an alternating magnetic field was calculated calorimetrically by registering the temperature increase in the DI water containing the ferrite particles after applying the AC magnetic field [7]. Measurements were performed at 0.1–15 MHz in a field amplitude up to 110 A/m.

3. Results and discussion

The X-ray diffraction patterns of synthesized ferrite particles are shown in Fig. 2. Ferrites of Fe_3O_4, $Li_{0.5}Fe_{2.5}O_4$, $Ni_{0.65}Zn_{0.35}Cu_{0.1}Fe_{1.9}O_4$ and $Co_xNi_{1-x}Fe_2O_4$ were single phase with a spinel type crystal structure, whereas $Ba_{1-x}Sr_xFe_{12}O_{19}$ exhibited a hexagonal crystal structure. Particles synthesized by the sol–gel method exhibited high crystallinity, except for the Fe_3O_4 synthesized by coprecipitation.

The magnetic properties of the prepared ferrite particles are shown in Table 1 and Fig. 3. We selected the samples for the various coercivity values of ferrites. For $Co_{1-x}Ni_xFe_2O_4$ and $Ba_{1-x}Sr_xFe_{12}O_{19}$, the coercivity was increased in accordance with increasing level of the Ni^{2+}, Sr^{2+} substitution. $Ni_{0.65}Zn_{0.35}Cu_{0.1}Fe_{1.9}O_4$ shows with 73.36 emu/g the greatest saturation magnetization in this experiment. However, the maximum hysteresis area was shown for $SrFe_{12}O_{19}$, which has the hexagonal structure and the highest coercivity. The difference of hysteresis area was approximately 0.7–0.9, as calculated by the hysteresis area ratio (hysteresis area of sample/hysteresis area of Sr-ferrite). The particle sizes for the samples presented in this study are shown in Table 1. The size was determined using SEM observation. It is known that the hysteresis loss is

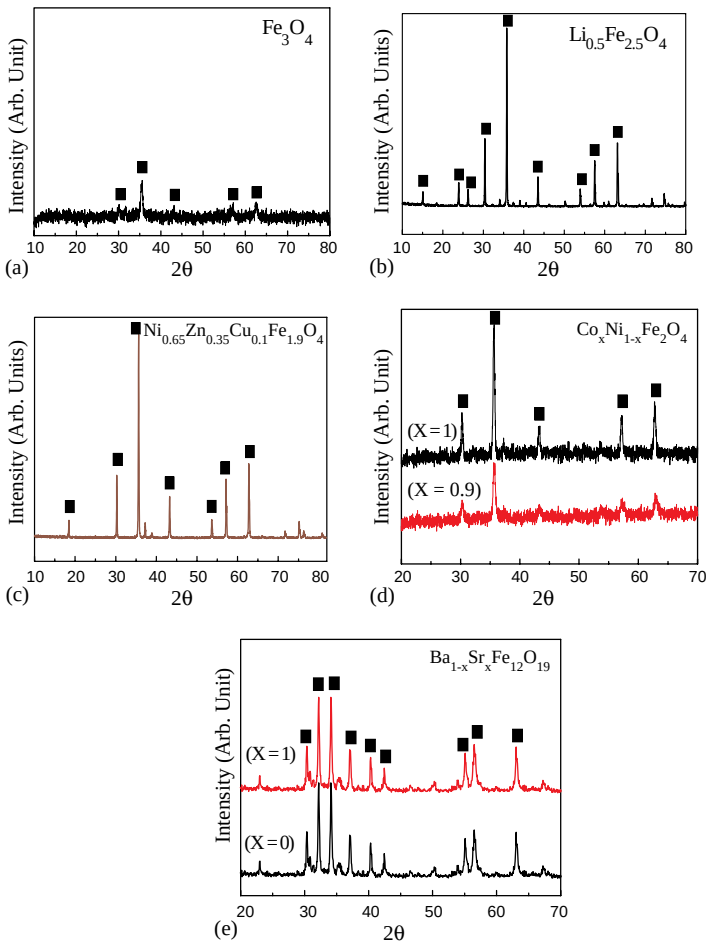

Fig. 2. XRD patterns of the ferrite particles (a) Fe_3O_4, (b) $Li_{0.5}Fe_{2.5}O_4$, (c) $Ni_{0.65}Zn_{0.35}Cu_{0.1}Fe_{1.9}O_4$, (d) $Co_xNi_{1-x}Fe_2O_4$ and (e) $Ba_{1-x}Sr_xFe_{12}O_{19}$.

Table 1
Particle sizes and magnetic properties of ferrite sample

Samples	Particle diameter (μm)	Coercivity H_c (Oe)	Magnetization M_s (emu/g)	Hysteresis area ratio
Fe_3O_4	0.10	64.55	45.75	0.08
$BaFe_{12}O_{19}$	0.42	5300.61	67.39	0.77
$SrFeO_{19}$	0.45	7054.24	70.54	1.00
$CoFe_2O_4$	0.17	326.78	72.09	0.11
$Co_{0.9}Ni_{0.1}Fe_2O_4$	0.22	376.01	67.78	0.13
$Li_{0.5}Fe_{2.5}O_4$	0.23	53.45	61.15	0.05
$Ni_{0.65}Zn_{0.35}Cu_{0.1}Fe_{1.9}O_4$	0.21	23.23	73.36	0.04

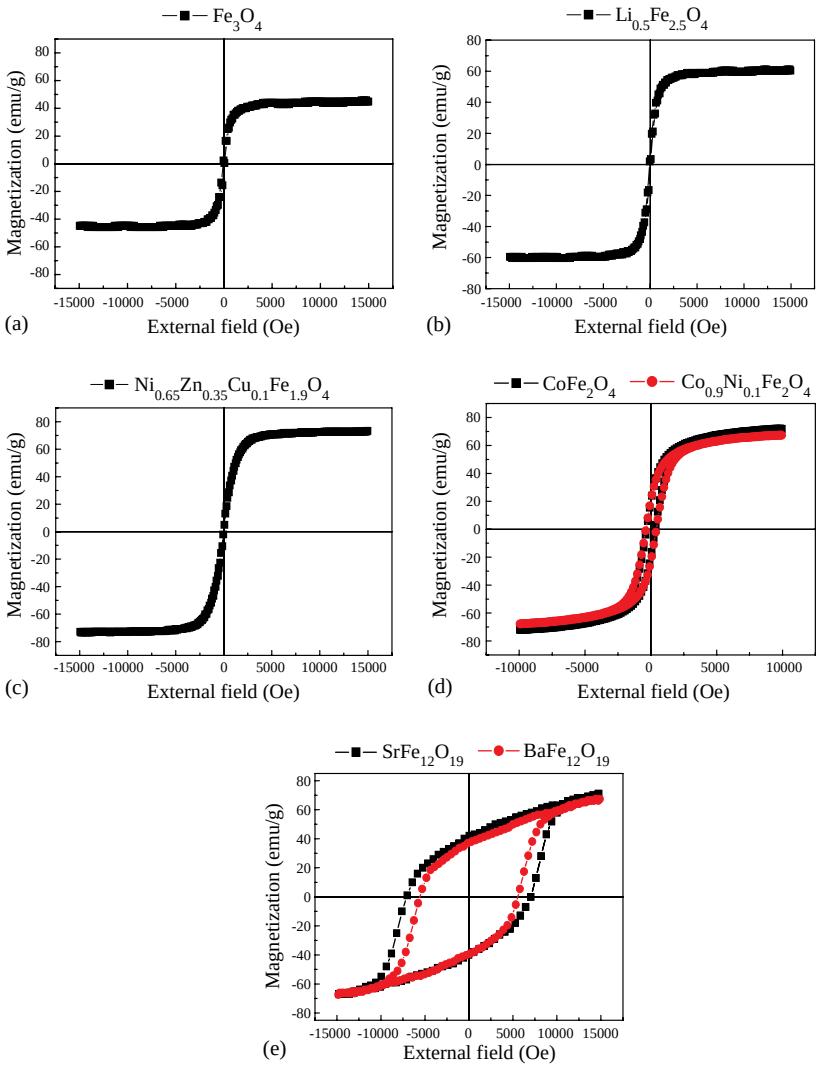

Fig. 3. Hysteresis loops of all samples (a) Fe_3O_4, (b) $Li_{0.5}Fe_{2.5}O_4$, (c) $Ni_{0.65}Zn_{0.35}Cu_{0.1}Fe_{1.9}O_4$, (d) $Co_xNi_{1-x}Fe_2O_4$ and (e) $Ba_{1-x}Sr_xFe_{12}O_{19}$.

strongly size dependent for nanosized particles [6]. In the present investigation, however, no relation could be observed between the magnetic properties and the particle size of the synthesized ferrites as shown in Table 1. This might be due to the relatively large, micrometer-sized range of the synthesized ferrites. However, the main contribution arises from the hysteresis loss and this is strongly size dependent for those particles of nano scale size [6].

The suitable frequency for the heating applicator was not all the frequencies (0.1–15 MHz) in this experiment. The prepared ferrite particles were exposed to an external alternating magnetic field of 6.77 and 7 MHz for measurement of the heat generation. Fig. 4 shows the time-dependent heating properties under the alternating magnetic field at 6.77 and 7 MHz for Fe_3O_4, $Li_{0.5}Fe_{2.5}O_4$, $Ni_{0.65}Zn_{0.35}Cu_{0.1}Fe_{1.9}O_4$, $CoFe_2O_4$, $Co_{0.9}Ni_{0.1}$-Fe_2O_4, $BaFe_{12}O_{19}$ and $SrFe_{12}O_{19}$ particles in

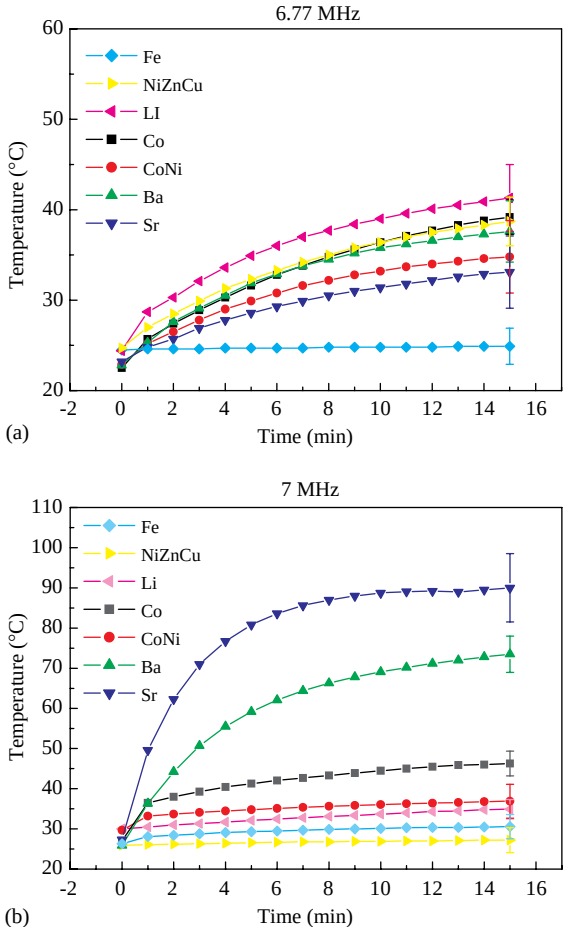

Fig. 4. Time-dependent temperature curves of samples in (a) 6.77 MHz and (b) 7 MHz AC magnetic field. (Fe—Fe_3O_4, Li—$Li_{0.5}Fe_{2.5}O_4$, NiZnCu—$Ni_{0.65}Zn_{0.35}Cu_{0.1}Fe_{1.9}O_4$, Co—$CoFe_2O_4$ CoNi—$Co_{0.9}Ni_{0.1}Fe_2O_4$ Ba—$BaFe_{12}O_{19}$ and Sr—$SrFe_{12}O_{19}$.)

water. The water temperature was increased by the ferrite particles when we applied the alternating magnetic field. Increasing the exposure time in the alternating magnetic field decreased the rate of temperature increase. When $Li_{0.5}Fe_{2.5}O_4$ particles were exposed to an alternating magnetic field of 6.77 MHz, the temperature change was measured as $\Delta T = 16.9$ K after 15 min. However, when we considered the sample weight, $CoFe_2O_4$ particles were calculated as having the highest SLP of 30.36 W/g s by measuring the temperature changes. The demand for high SLP is given by economical considerations. It was difficult to compare the different materials as data were measured for different values of field amplitude and frequency. Being exposed to an alternating magnetic field with 7 MHz, $SrFe_{12}O_{19}$ particles were calculated by using the temperature changes, as having the highest SLP (96.46 W/g s). The increases in temperature for $SrFe_{12}O_{19}$ and $BaFe_{12}O_{19}$ were considerably higher than for those of other ferrite particles.

SLP in the low frequency of 6.77 MHz was increased in ferrite particles which have lower coercivity than Ba- or Sr-ferrite but this is in accordance with the area of hysteresis, that is, SLP values were increased in 7 MHz. These results are explained by the hysteresis loss. In the case of Ba- and Sr-ferrite particles, which had the high coercivity, by using low-field amplitudes, you rarely can change the magnetization direction of the single domain particles that has high shape anisotropy. Unfortunately, there are considerable problems with the application of high amplitude alternating magnetic fields to a human patient [8]. The heating of magnetic particles with a low-electrical conductivity in an external alternating magnetic field is mainly due to a loss process during the reorientation of the magnetization. The SLP for $CoFe_2O_4$, $Co_{0.9}Ni_{0.1}Fe_2O_4$, $Li_{0.5}Fe_{2.5}O_4$ and $Ni_{0.65}Zn_{0.35}Cu_{0.1}Fe_{1.9}O_4$ particles was not increased with the frequency. In these samples (i.e. having the low coercivity), which consist at least partially of multidomain particles, one may assume that the mechanical work, that the ferrite particles have undergone during preparation, resulted in domain wall pinning centers, that already caused relatively high losses at low-field amplitude [8]. For the effective heat generation in ferrite particles, the determination of a suitable frequency and magnetic field is very important. The SLP of ferrite particles in an external alternating magnetic field can be attributed to two kinds of power loss mechanisms—hysteresis loss and relaxation loss. The coercivity (H_c) is the main technical parameter to characterize the magnetism of ferrite particles. The coercivity is strongly size dependent [9]. In bulk samples whose sizes exceed the domain wall width, magnetization

Table 2
Temperature and SLP of ferrite particles under the AC magnetic field (6.77 and 7 MHz) for 15 min

Samples	6.77 MHz		7 MHz	
	ΔT (K)	SLP (W/g s)	ΔT (K)	SLP (W/g s)
Fe_3O_4	0.40	0.62	4.30	6.62
$BaFe_{12}O_{19}$	14.80	22.77	47.60	73.23
$SrFeO_{19}$	9.90	15.23	62.70	96.46
$CoFe_2O_4$	16.70	30.36	19.25	29.62
$Co_{0.9}Ni_{0.1}Fe_2O_4$	11.90	18.31	7.20	11.08
$Li_{0.5}Fe_{2.5}O_4$	16.90	13.52	4.90	4.92
$Ni_{0.65}Zn_{0.35}Cu_{0.1}Fe_{1.9}O_4$	14.00	11.20	1.30	1.33

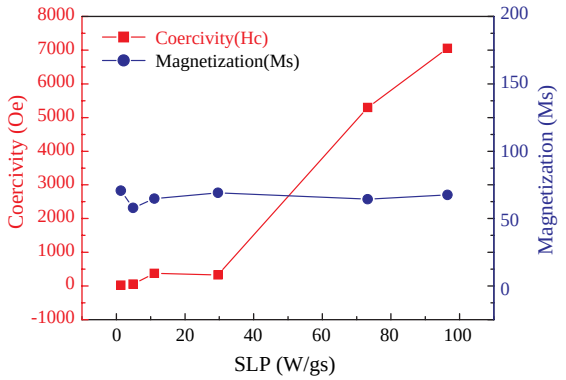

Fig. 5. Coercivity H_c and magnetization M_s as functions of the values of SLP.

reversal occurs due to domain wall motion. As domain walls move through a sample, they can become pinned at grain boundaries and additional energy is needed for them to continue moving. Pinning is one of the main sources of the coercivity [10]. As we increased the coercivity of the ferrite particles, the SLP values were also increased (Table 2). In Fig. 5, as increasing the coercivity and hysteresis area, the value of SLP was increased.

Ferrite particles within alternating magnetic field are expected to be useful thermoseeds in hyperthermic cancer treatment since they can be targeted and confined to the cancer site. Too high SLP value in Ba- and Sr-ferrite ($\Delta T = 47.6$, 62.7 K at 7 MHz (110 kA/m)) particles is damaging to normal cells. Above the temperature of 42–45 °C, both cellular membranes and nuclear structures are damaged by heat and can be important in the lethality from heat [11]. In this study, $CoFe_2O_4$ particles show a good SLP value when applying a hyperthermic temperature of 42–45 °C for 15–20 min.

4. Conclusion

Various ferrite particles with different magnetic properties were prepared with the sol–gel method and their heating properties were measured by a heating system using an alternating magnetic field generator and amplifier. We studied the applicability of ferrite particles for their hysteresis loss in heating hyperthermia at various frequencies.

The areas of hysteresis loops were much larger for Ba- and Sr- ferrites than that of the Fe-, Li-, Ni/Zn/Cu-, Co-, Co/Ni-ferrites. The heating ability of each ferrite increased with an increase of the alternating magnetic field. Among these ferrites, Co-ferrite exhibited the temperature change, $\Delta T =$ 19.25 K, in distilled water when the field was 110 A/m. At that time, the specific loss power of Co-ferrites was 29.62 W/g s. We need the best ferrite to heat more efficiently in tumor without damaging normal cells in a low magnetic field. Therefore, Co-ferrite would be effective as thermoseeds for hyperthermia under the alternating magnetic field.

Acknowledgements

This work was supported by Grant No. R01-2001-000-00157 from the Basic Research Program of the Korea Science & Engineering Foundation.

References

[1] J.B. Goodenough, IEEE Trans. Magn. 38 (2002) 3398.
[2] F. Sato, M. Jojo, H. Matsuki, et al., IEEE Trans. Magn. 38 (2002) 3362.
[3] J.J. Breedlove, W.H. Newman, G.T. Martin, et al., IEEE EMBC & CMBEC 2 (1995) 1521.
[4] Y.H. Mier, A.V. Hernandez, L.L. Salas, Proceedings of the Second Joint EMBS/BMES Conference (2002).
[5] D.C.F. Chan, D.B. Kirpotin, P.A. Bunn, J. Magn. Magn. Mater. 122 (1993) 374.
[6] M. Ma, Y. Wu, J. Zhou, et al., J. Magn. Magn. Mater. 268 (2004) 33.
[7] R. Hergt, R. Hiergeist, I. Hilger, W.A. Kaiser, Y. Lapatnikov, S. Margel, U. Ritcher, J. Magn. Magn. Mater. 270 (2004) 345.
[8] R. Hergt, W. Andrä, C.G. d'Ambly, et al., IEEE Trans. Magn. 34 (1998) 3745.
[9] G. Herzer, IEEE Trans. Magn. 26 (1990) 1397.
[10] G. Herzer, J. Magn. Magn. Mater. 112 (1992) 258.
[11] S.P. Thomasovic, Tenth Annual International Conference 0861, IEEE Eng. Med. Biol. Magn. (1988).